

A 108769

J. Short
323-213

NSWC TR 79-485

PARAMETRIC STUDY OF PROPELLANT CRACK COMBUSTION

BY KIBONG KIM

RESEARCH AND TECHNOLOGY DEPARTMENT

21 OCTOBER 1981

20060608063

Approved for public release, distribution unlimited



NAVAL SURFACE WEAPONS CENTER

Dahlgren, Virginia 22448 • Silver Spring, Maryland 20910

UNCLASSIFIED

SECURITY CLASSIFICATION OF THIS PAGE (When Data Entered)

REPORT DOCUMENTATION PAGE		READ INSTRUCTIONS BEFORE COMPLETING FORM
1. REPORT NUMBER NSWC TR 79-485	2. GOVT ACCESSION NO.	3. RECIPIENT'S CATALOG NUMBER
4. TITLE (and Subtitle) PARAMETRIC STUDY OF PROPELLANT CRACK COMBUSTION		5. TYPE OF REPORT & PERIOD COVERED Final Report FY1979
		6. PERFORMING ORG. REPORT NUMBER
7. AUTHOR(s) Kibong Kim		8. CONTRACT OR GRANT NUMBER(s)
9. PERFORMING ORGANIZATION NAME AND ADDRESS Naval Surface Weapons Center White Oak, Silver Spring, Maryland 20910		10. PROGRAM ELEMENT, PROJECT, TASK AREA & WORK UNIT NUMBERS 64363N; HEPS; B0003-001/77402; 9R13DA
11. CONTROLLING OFFICE NAME AND ADDRESS Strategic Systems Project Office Washington, D. C. 20376		12. REPORT DATE 21 October 1981
		13. NUMBER OF PAGES 38
14. MONITORING AGENCY NAME & ADDRESS (if different from Controlling Office)		15. SECURITY CLASS. (of this report) UNCLASSIFIED
		15a. DECLASSIFICATION/DOWNGRADING SCHEDULE
16. DISTRIBUTION STATEMENT (of this Report) Approved for public release; distribution unlimited.		
17. DISTRIBUTION STATEMENT (of the abstract entered in Block 20, if different from Report)		
18. SUPPLEMENTARY NOTES		
19. KEY WORDS (Continue on reverse side if necessary and identify by block number) Crack, Propellant, Combustion, Transition-to-Detonation		
20. ABSTRACT (Continue on reverse side if necessary and identify by block number) Selective calculations have been made for burning in cracks as it pertains to solid rocket motor propellants. The possibility of obtaining pressures high enough to cause a shock-to-detonation transition (SDT) in propellant grains is examined. Variables affecting the crack combustion process which were selected for study are: crack shape; location; surface roughness; propellant deformation; ignition criterion; and burning rate. The variables are evaluated and ordered in groups of relative importance. Results		

DD FORM 1473
1 JAN 73EDITION OF 1 NOV 65 IS OBSOLETE
S/N 0102-LF-014-6601

UNCLASSIFIED

SECURITY CLASSIFICATION OF THIS PAGE (When Data Entered)

UNCLASSIFIED

SECURITY CLASSIFICATION OF THIS PAGE (When Data Entered)

20. (cont.) suggest that SDT should not occur in propellants unless the granulation of the grain is severe enough to provide large burning surface area.

UNCLASSIFIED

SECURITY CLASSIFICATION OF THIS PAGE (When Data Entered)

FOREWORD

Selective calculations have been made for burning in cracks as it pertains to solid rocket motor propellants. The possibility of obtaining pressures high enough to cause a shock-to-detonation transition (SDT) in propellant grains is examined. Variables affecting the crack combustion process which were selected for study are: crack shape, location, surface roughness, propellant deformation, ignition criterion, and burning rate. The variables are evaluated and ordered in groups of relative importance. Results suggest that SDT should not occur in propellants unless the granulation of the grain is severe enough to provide large burning surface area.


J. F. PROCTOR
By direction

CONTENTS

	<u>Page</u>
INTRODUCTION	5
IDENTIFICATION OF IMPORTANT PARAMETERS	7
EVALUATION OF PARAMETERS	9
IGNITION CRITERION	16
SIMILARITY	16
PROPELLANT DEFORMATION	16
ROUGH SURFACE, HIGH BURNING RATES	20
CONCLUSIONS	24
REFERENCES	25
APPENDIX A - CRACK COMBUSTION CODE (KUO)	A-1

ILLUSTRATIONS

<u>Figure</u>		<u>Page</u>
1	SCHEMATIC CRACK BURNING PROCESS	8
2	CALCULATED PRESSURE PROFILES AT VARIOUS TIME -- BASELINE CASE I	11
3	TEMPERATURE PROFILES AT VARIOUS TIMES -- BASELINE CASE I.	12
4	VELOCITY PROFILES -- BASELINE CASE I.	13
5	CRACK WIDTH -- BASELINE CASE I.	14
6	PRESSURE PROFILES, BASELINE CASE II -- CRACK WIDTH IS 3/10 TIMES SMALLER THAN THE BASELINE CASE I	15
7	PRESSURE PROFILES -- LOWER IGNITION TEMPERATURE THAN THE BASELINE CASE I	17
8	PRESSURE PROFILES -- SIMILAR-SHAPED CRACK AS THE BASELINE CASE I BUT 3/10 TIMES SMALLER.	18
9	IDEALIZED SINGLE CRACK GEOMETRY IN MULTIPLE CRACK SITUATION	19
10	PRESSURE-DISTANCE PROFILE AT VARIOUS TIMES WITH PROPELLANT DEFORMATION	21
11	PRESSURE PROFILE WITH PROPELLANT DEFORMATION, $\alpha = 2$	22
12	PRESSURE PROFILE WITH PROPELLANT DEFORMATION, $\alpha = 3$	23

TABLES

<u>Table</u>		<u>Page</u>
1	INPUT PARAMETERS USED FOR SIMULATION.	10

INTRODUCTION

Even though qualified solid rocket motors have failed due to fires, case bursts and nozzle expulsions, no service motor detonated prior to 1975¹. The record is quite impressive considering that the knowledge of solid rocket motors is primarily empirical. One reason is that the propellants used were of moderate performance and their mechanical strength was good.

However, propellants under development since 1975 for high performance rocket motors contain ingredients which are more detonable including combustible fillers and binders. This increases the general sensitivity of the propellants in the solid content (decrease in binder content) of propellants which can result in poor mechanical properties and increased sensitivity. In fact, several motors made of such high energy propellants detonated high order during development.

These failures have been carefully investigated and there are several possible scenarios presented²:

- a. Shear. Damage in the propellant-to-chamber bond region creating a bed of damaged propellant having sufficient granulation, cleavage and confinement to support a series of events leading to deflagration-to-detonation transition (DDT).
- b. Impact. Detonation of expelled propellant fragments on nearby objects leading to shock-to-detonation transition (SDT) by sympathetic reaction from these expelled fragment reactions to the propellant bulk.

¹J. F. Kincaid and S. J. Jacobs, "The Fundamentals of High Energy Propellant Safety," Report No. 10342.1 SP-20 CON., Dept. of Navy, Strategic Systems Project Office, 1975.

²J. M. Anderson, J. H. Thacher and R. B. Wetherell, "Trident Motor Detonation Studies: An Overview," Presented at the 15th JANNAF Combustion Meeting, Rhode Island, 1978.

c. Implosion.

1. Implosion-DDT, wherein the grain failed near the case bond and is deflected inward by high pressure at its periphery, causing breakup or cracking in the centerport, leading to DDT.
2. Implosion-SDT, wherein the grain collapse is sufficiently rapid to create high internal shock loads at the centerport, leading into SDT.

Given these scenarios, attempts have been made to analyze them theoretically and in laboratory experiments by delineating and examining the essential features in detail. Studies include DDT in granular beds³, DDT and SDT in both cast and pressed explosives⁴, cracks⁵, and impacts⁶.

The studies also include the investigation of convective burning processes in propellant cracks. It is known that small cracks exposed to rocket motor chamber provide more surface area thereby increasing the chamber pressure. There are many experimental works on the subject⁷.

Kuo⁸ developed a one-dimensional combustion model simulating ignition and combustion in solid propellant cracks with variable cross section along the length of the crack. Results of the model analysis agreed with some experimental evidence at low pressures. However, although these studies concentrated on "flashdown", a flame propagation into a crack, they did not consider the possibility of obtaining high enough pressure in the crack to initiate a DDT in propellants.

³B. D. Hopkins, N. L. Peterson, M. W. Beckstead, D. T. Pilcher and A. G. Butcher, "Mathematical Modeling of the DDT Process," Presented at the 15th JANNAF Combustion Meeting, Rhode Island, 1978.

⁴C. A. Forest, "Numerical Modeling of the Deflagration-to-Detonation Transition," Presented at the 15th JANNAF Combustion Meeting, Rhode Island, 1978.

⁵J. L. Prentice, "Onset of Convective Combustion: Flashdown in Solid Propellants," Presented at the 15th JANNAF Combustion Meeting, Rhode Island, 1978.

⁶R. C. Jensen, "Investigation of High Velocity Impact Initiated Detonations," Presented at the 15th JANNAF Combustion Meeting, Rhode Island, 1978.

⁷A. F. Belyaev, F. K. Bobolev, A. I. Korotkov, A. A. Sulimov, and G. V. Chuiko, Transition From Deflagration to Detonation In Condensed Explosives, Israel Program for Scientific Translations, Jerusalem, 1975.

⁸K. K. Kuo, A. T. Chen and T. R. Davis, "Convective Burning in Solid Propellant Cracks," AIAA J., Vol. 16, No. 6, 1978.

The objective of this report is to evaluate the possibility of initiating high order detonation in propellants through crack burning. It is a very complex task in the sense that no set of definite approaches is available, making it difficult to carry out systematic experimental study. Furthermore, parameters in the problem (for example, crack shapes and propellant burning rate), are interdependent and add more complexity.

In this report, the following approaches are taken. First, factors which affect the crack burning process are identified. These factors should include propellant material properties as well as crack geometry. Then the factors are tested for their relative importance in the pressurization process in burning cracks. For this purpose, Kuo's crack combustion model was modified to include the effect of surface roughness and propellant deformation.

IDENTIFICATION OF IMPORTANT PARAMETERS

Consider a simplified crack combustion system shown in Fig. 1. An amplified view of a crack is shown to face the rocket chamber filled with hot, high pressure gas. The hot gas initially penetrates into the crack cavity, heating the propellant surface through convective heat transfer. Some of the heat is lost through conductive heat transfer into the propellant body. If the convective heat transfer is higher than the heat loss through conductive heat transfer, the surface temperature increases until it reaches the ignition temperature of the propellant. When ignited, the propellant burns at a rate dependent on the local gas pressure whose rate of buildup depends on the burning rate and the geometry of the crack. A rough surface provides a large burning area and hence a large gasification rate. As the burning rate increases, a compressive wave is formed which enters and propagates along the crack ahead of the flame front (ignition front). The crack cavity is further pressurized by the gasification of the solid propellant and by reflection of the compression wave at the end of the crack. The pressurization continues until the crack width is sufficiently enlarged by consumption of propellant so that the gas escape rate through the crack opening is larger than the gas generation rate inside the crack. In the current discussion, crack propagation (increase of crack length) is not considered.

The crack combustion system can be analyzed by solving a set of partial differential equations (conservation equations for gas phase) with appropriate initial and boundary conditions, containing non-homogeneous mass, momentum and energy source terms. Parameters which influence the crack combustion process are:

- a. Geometry. There are several independent parameters describing the geometry of the crack. These are the crack length, L , the crack width, W , and the roughness of the crack's inner surface. Small cracks may branch off the main crack to provide additional surface area for combustion. Also, the deformation of the propellant due to the gas pressure in the crack plays an important role in the crack combustion process.

- b. Initial Conditions (T_0, p_0). In most cases, initial conditions inside the crack are not important to the crack combustion process. The initial pressure is small compared to the chamber pressure and does not present significant resistance to the hot chamber gas penetration into the crack.
- c. Boundary Conditions. The boundary conditions are:
1. The pressure at the inlet of the crack equals the chamber pressure or there exists a choked flow condition at the crack inlet.
 2. The gas velocity at the closed crack's end is zero.

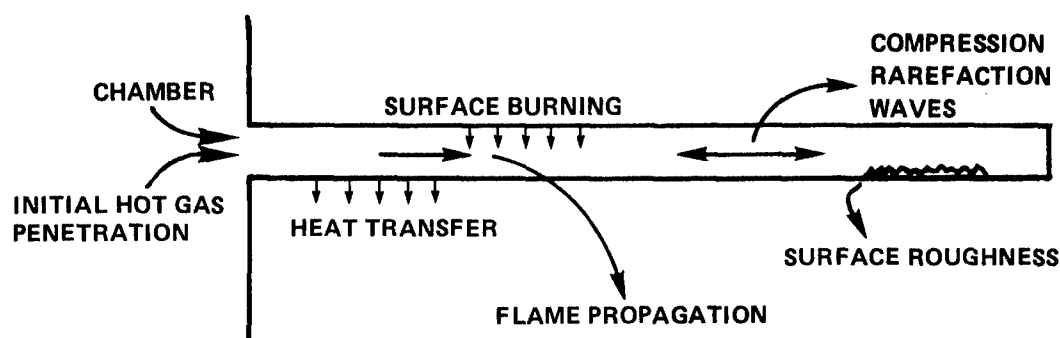


FIGURE 1 SCHEMATIC CRACK BURNING PROCESS

If the crack is initially exposed to the rocket chamber when the rocket motor is being ignited, then the chamber pressure (crack inlet boundary condition) is a slowly increasing function of time until it reaches a motor operating pressure (arbitrarily chosen here to be about 10 MPa). The characteristic time scale is of the order of 0.1 seconds. Kuo⁸ has shown that under this condition, the pressure in the crack is almost identical to the chamber pressure, indicating that there is no additional pressure buildup due to the presence of the crack. For this reason, the case where the crack is initially exposed to the rocket chamber is not discussed here. The cracks considered are those suddenly opened to the already established chamber pressure of 10 MPa (embedded cracks with one side of the crack being exposed to rocket chamber pressure by burning of the propellant) or - suddenly created due to mechanical failure. The boundary condition (1) stated above is modified in this case as follows:

1. The pressure at the inlet of the crack is 10 MPa or there exists a choked flow condition at the crack inlet.

- d. Ignition and Burning Characteristics of Propellants. Burning characteristics of the propellants also contributes to the pressurization process as in solid propellant rocket motors in which burning rate and rocket motor geometry together establish a stable operating chamber pressure. Although ignition characteristics are not important in rocket motors because the ignition delay time is relatively short compared to the burning time to maximum pressure, they will be considered in this paper because the characteristic time in the crack combustion process may be of the same order of magnitude as the ignition delay time.

In the following treatment, only items (a) and (d) of the above will be studied. As discussed in the INTRODUCTION, it is impossible to evaluate all parameters in a comprehensive way because of the nonlinearities of the problem and the interdependency of the parameters. The approach chosen in this paper is to examine each parameter singly and establish its importance with a modification of Kuo's Crack Combustion Code. The code is explained in detail in the Appendix.

EVALUATION OF PARAMETERS

BASELINE CASE

Initial crack shape was studied first disregarding propellant deformation. Two cases are considered for the geometrical effects. Parameters used are listed in Table 1. The length to width ratio of the crack, L/W , is about 300 in Case I, and 1000 in Case II.

Case I. The details of the crack combustion process computed by Kuo's model are illustrated in Figs. 2-5 for Case I and compared with Fig. 6 for Case II. Fig. 2 shows a $p-x$ diagram at various times for Case I. $x = 0$ at the crack entrance and $x = L = 15.05$ cm at the crack tip. As stated previously, the chamber pressure is maintained at 100 bars (10 MPa). Note that the initial pressure wave travels for about 150 μsec before it is reflected at the crack tip. Dashes on the $p-x$ profiles for 50 ~ 150 μsec indicate the position of flame front (or ignition front) at these times. The figure therefore shows that the ignition front follows the pressure wave front closely and, at about 150 μsec , the entire crack is ignited. The pressure at the time is more or less constant throughout the length of the crack but steadily increases as the wave is reflected from the crack tip. Even after a rarefaction wave comes into the crack after 300 μsec , this pressurization continues. Pressurization will continue until the crack width is sufficiently enlarged for the mass generation rate in the crack to equal the rate of mass escape out of the crack. The pressure peak will be discussed further when propellant deformation is studied.

TABLE 1 INPUT PARAMETERS USED FOR SIMULATION

W = crack width = 0.0508 cm for Case I, and = 0.015 cm for Case II

L = crack length = 15.05 cm

B_x = Body force = 0.0 g_f/g

b = co-volume = 1.0 cm³/g

M_w = molecular weight = 23.97 g/gr-mole

γ = specific heat ratio = 1.233

ρ_{pr} = propellant density = 1.741 g/cm³

λ_{pr} = thermal conductivity = 0.55 x 10⁻³ cal/sec-cm-°K

α_{pr} = thermal diffusivity = 0.001 cm²/sec

ϵ_r = relative roughness

= surface roughness/hydraulic diameter of the crack = 0.001

T_f = flame temperature = 3000°K

T_{cri} = critical temperature = 780°K

T_{ign} = ignition temperature = 1000°K

T_i = initial temperature = 298°K

a = pre-exponential factor
in burning rate law = 2.752 x 10⁻⁴ (cm/sec)/(g/cm²)ⁿ

n = exponent = 0.683

K_e = erosive burning constant = 15.9 cm³ - °K/cal

β = erosive burning exponent = 125

T_c = chamber temperature = 2800°K

P_c = chamber pressure = 100 bars for $t \geq 0$

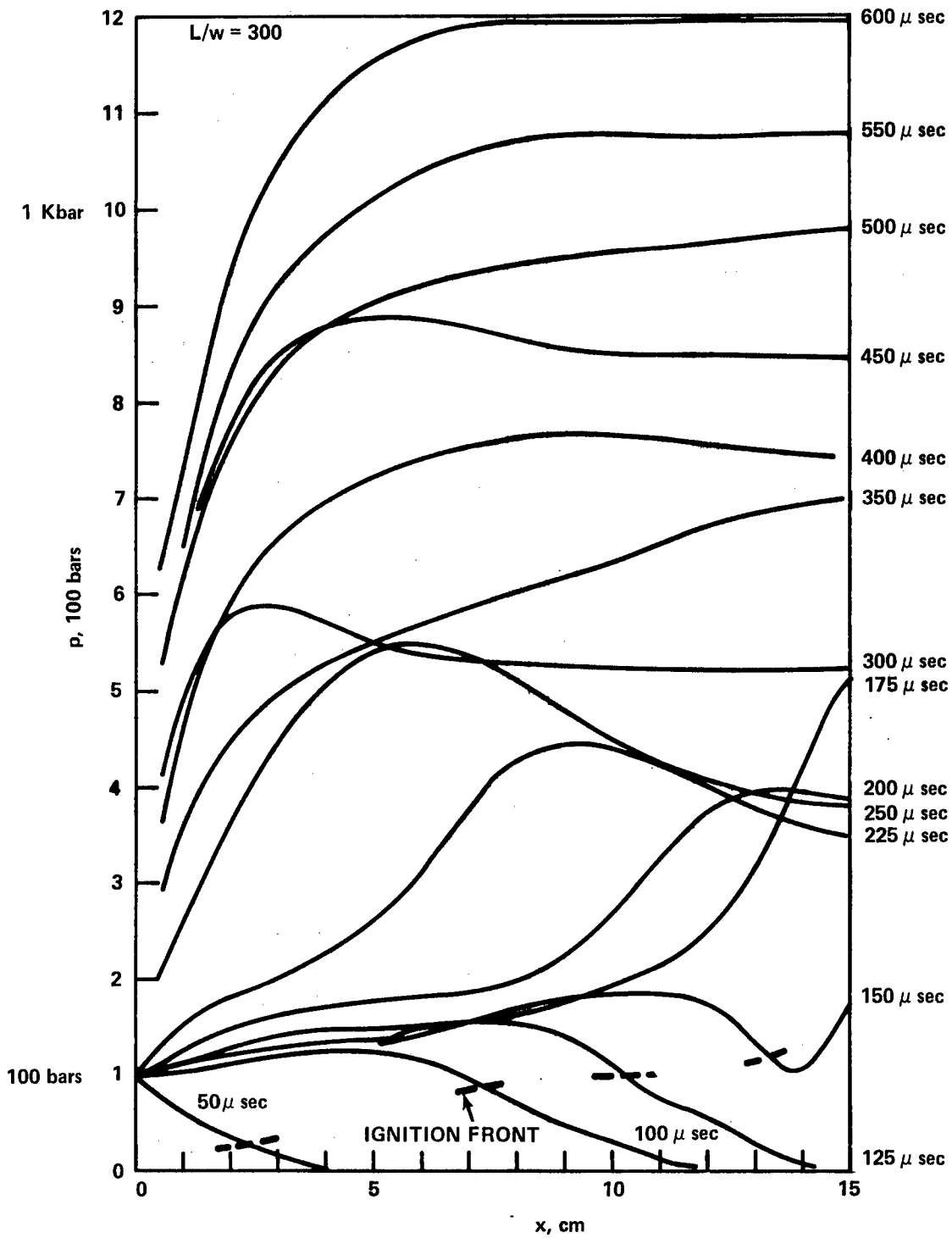


FIGURE 2 CALCULATED PRESSURE PROFILES AT VARIOUS TIME --- BASELINE CASE I. IGNITION FRONT IS SHOWN AT BOTTOM OF THE FIGURE.

Figure 3 shows the gas temperature profile. It increases from the initial value of 298°K to around 3000°K as the first compression wave propagates into the crack and the temperature remains approximately constant throughout the process. One exception of this is that at the end of the crack, the cold gas which was initially in the crack is less than 3000°K although it is compressed at the end of the crack to form a cool pocket in that region.

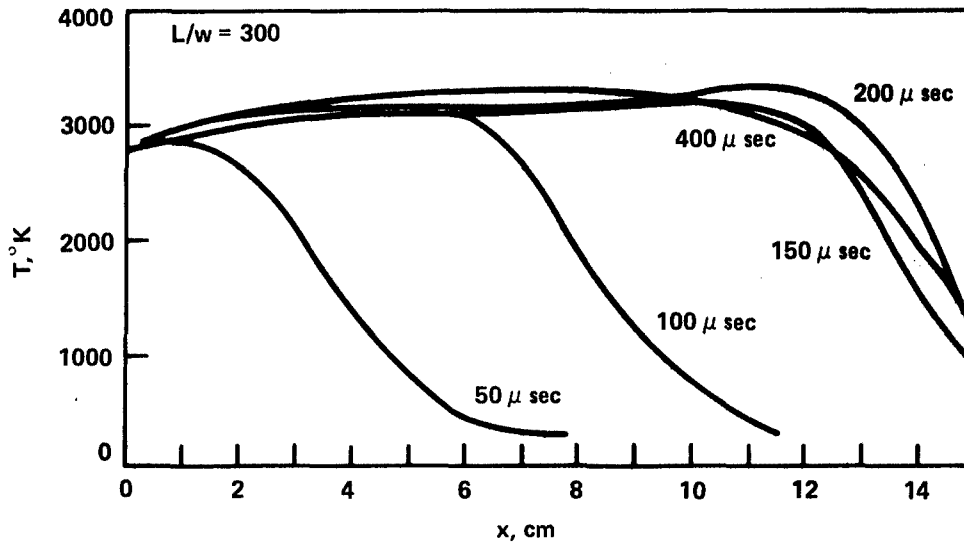


FIGURE 3 TEMPERATURE PROFILES AT VARIOUS TIMES --- BASELINE CASE I

Gas velocity profiles as a function of space at various times are depicted in Fig. 4. The initial compression wave traveling inward is evident from the positive velocity profiles at 50, 100 and 150 μsec . At 150 μsec , some part of the gas near the open end escapes to the chamber. At 300 μsec , the velocity of the bulk of the gas is almost at rest (in this particular case, slightly positive) and near the open end the gas is rushing out. From then on, the bulk of the gas maintains accelerating gas profiles toward the open end.

The change of the crack width in time is shown in Fig. 5. The original crack width is 0.0508 cm. The width increases fastest near the open end because that end is ignited first and because high gas velocity increases the erosive burning effect there (Refer to Fig. 4).

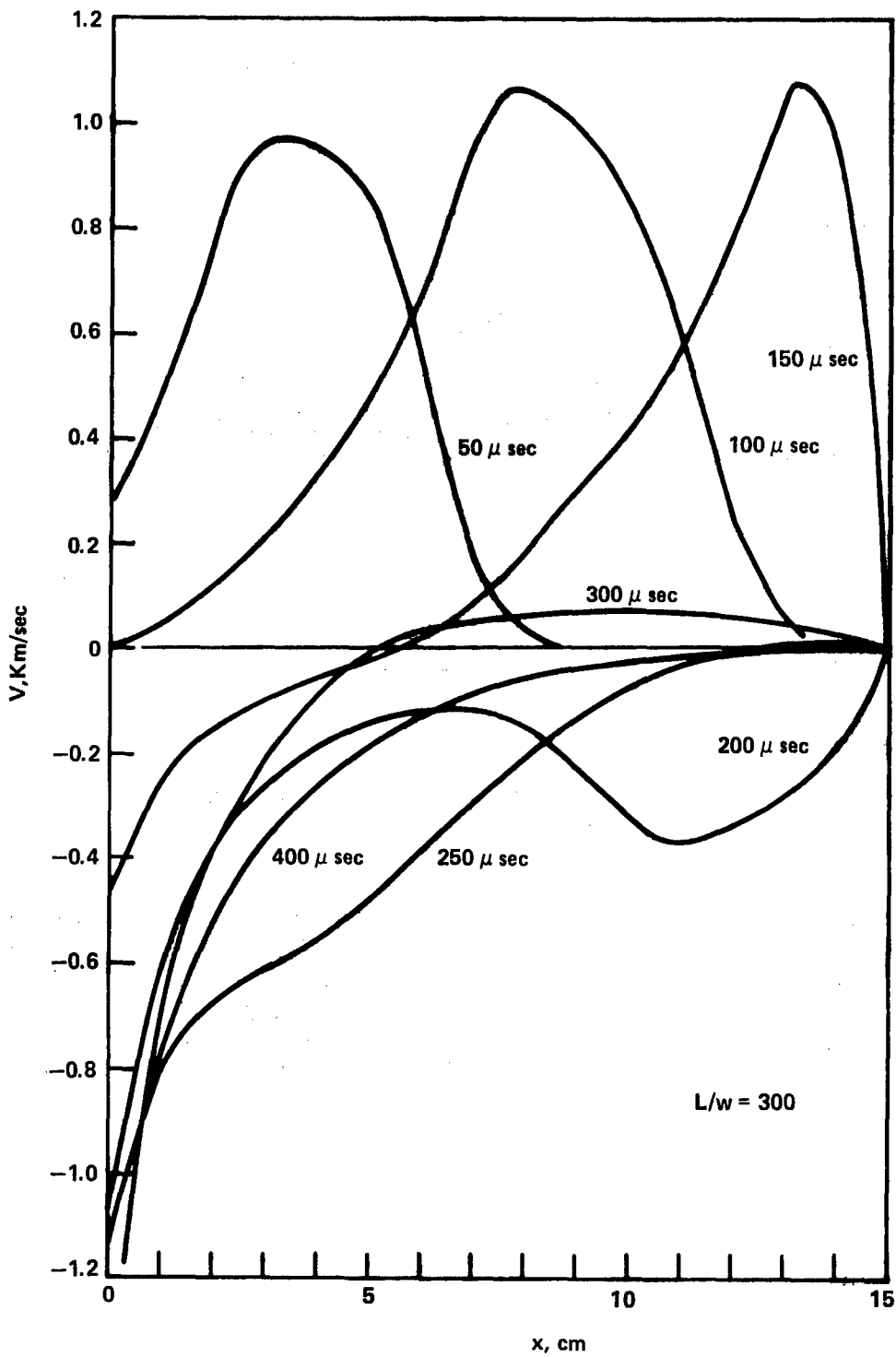


FIGURE 4 VELOCITY PROFILES --- BASELINE CASE I

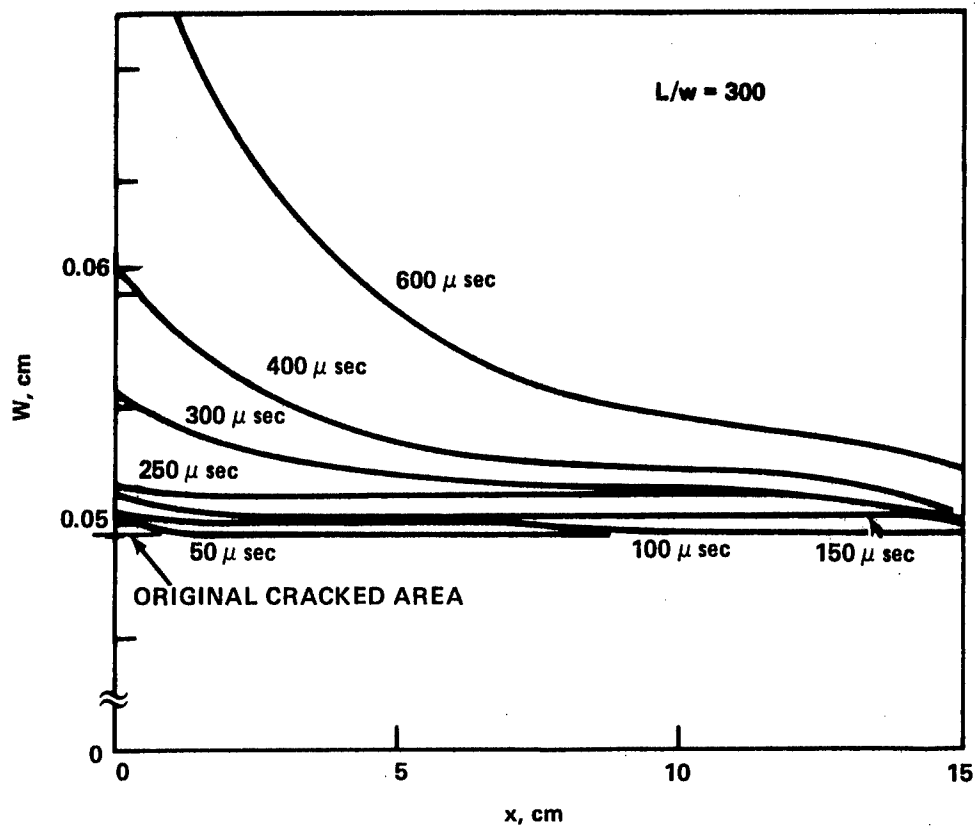


FIGURE 5 CRACK WIDTH --- BASELINE CASE I

Case II. Case II results are shown in Fig. 6 for comparison. L/W ratio for Case II is 1000 as compared to 300 for Case I. The figure displays $P-x$ profiles in the crack at various times as did Fig. 2. The smaller crack width (or the larger L/W) - increases the pressure in the crack significantly by the time the ignition first reached the crack's tip, the peak pressure has already exceeded 1 kbar and is rising rapidly (at 225 μ sec, the peak pressure is around 8 kbar). This illustrates the importance of the crack geometry in the pressurization of the crack.

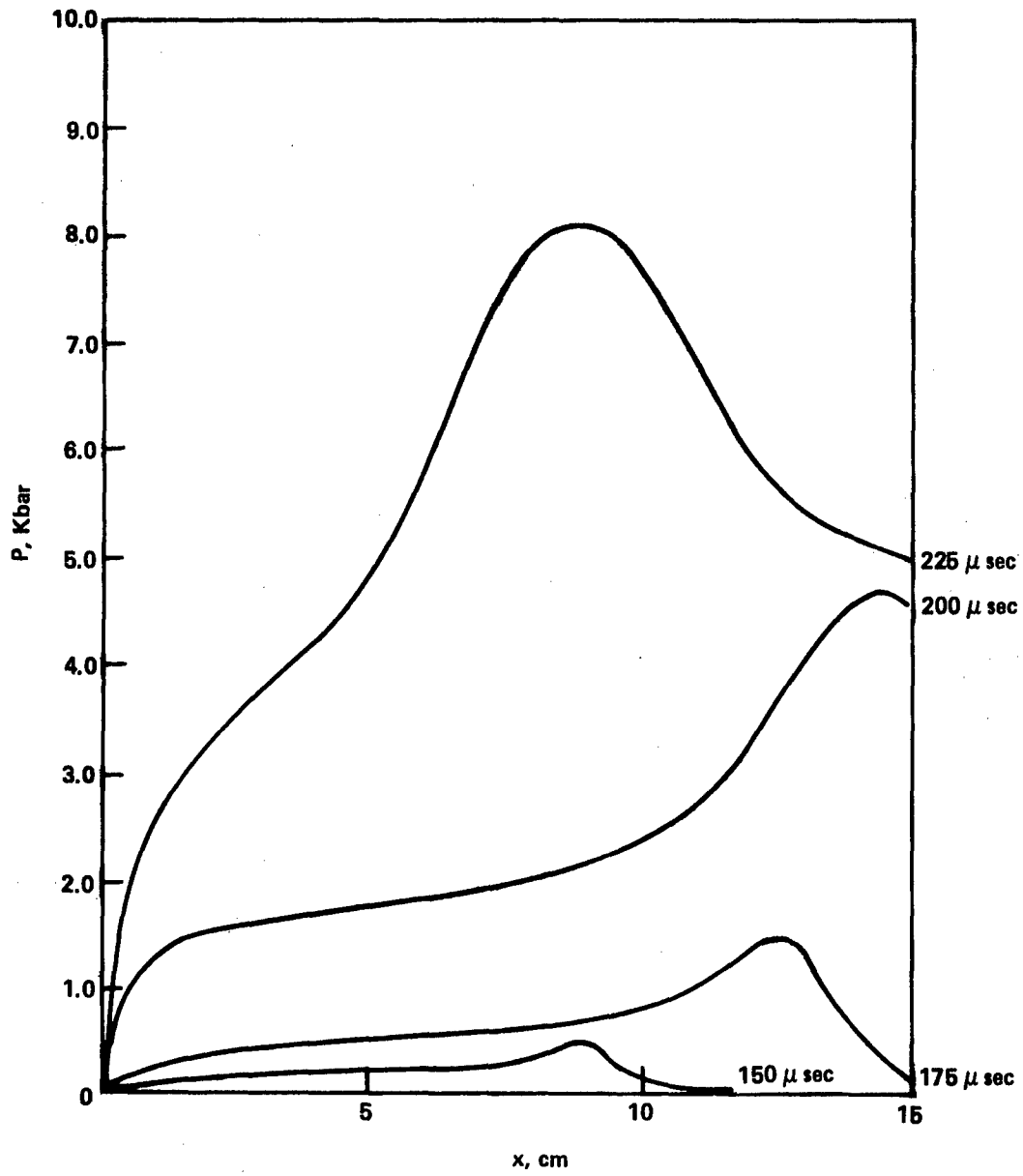


FIGURE 6 PRESSURE PROFILES, BASELINE CASE II --- CRACK WIDTH IS 3/10 TIMES SMALLER THAN THE BASELINE CASE I

IGNITION CRITERION

Results shown thus far indicate that the ignition front (or the flame front) closely follows the first compression wave propagating into the crack. Since the major pressurization in cracks occurs after the entire crack is ignited, moderate changes in ignition phase, or in ignition characteristics are not expected to change the crack combustion process significantly. This is shown in Fig. 7. The situation is identical to the baseline Case I except that the ignition temperature is lowered by 100°K. The trend is similar to the baseline case except that due to the choice of a lower ignition temperature, the first compression front propagates a little faster than in the baseline case. There is roughly a 25 μ sec gain which persists throughout the combustion process.

SIMILARITY

There has been an emphasis on the ratio L/W rather than on L or W separately in crack combustion studies⁹. When the pressurization in the crack is moderate at low L/W, the propellant deformation is not severe, and as the first compression wave into the crack is reflected from the crack tip, the crack is nearly uniformly pressurized and ignition is completed, the following processes depend entirely on fluid mechanics with the mass generation term dependent upon fluid dynamic variables only. The resulting partial differential equation describing the flow process from that point on can be scaled with L/W as long as thermodynamic variables in the crack are approximately constant when the ignition is completed. This deduction has been verified by examining Fig. 8 which is identical with Case I except that L and W are both 3/10 times smaller.

However, at high L/W, the uniform initial condition cannot be assumed after the compression wave is reflected at the crack tip as one observes a severe pressure gradient in the crack. Furthermore, propellant deformation plays a more important role in this case for a similarity to hold. Therefore, at high L/W ratio, L and W should be independently studied rather than a single parameter representation of L/W.

PROPELLANT DEFORMATION

The crack geometry is dependent upon many factors. The initial geometry is important, and as burning progresses, the increased width due to propellant consumption also plays a role. Another important factor is the increased width caused by high internal pressure deforming the propellant body surrounding the crack. The amount of the propellant deformation, or the enlargement of the crack, for a given propellant depends on the surrounding geometry. Consider a geometry shown in Fig. 9.

⁹A. T. Belyaev, A. I. Korotkov, A. A. Kulimov, M. K. Sukoyan and A. V. Obmenin, "Development of Combustion in an Isolated Pore," Combustion, Explosion and Shock Waves, Vol. 5.

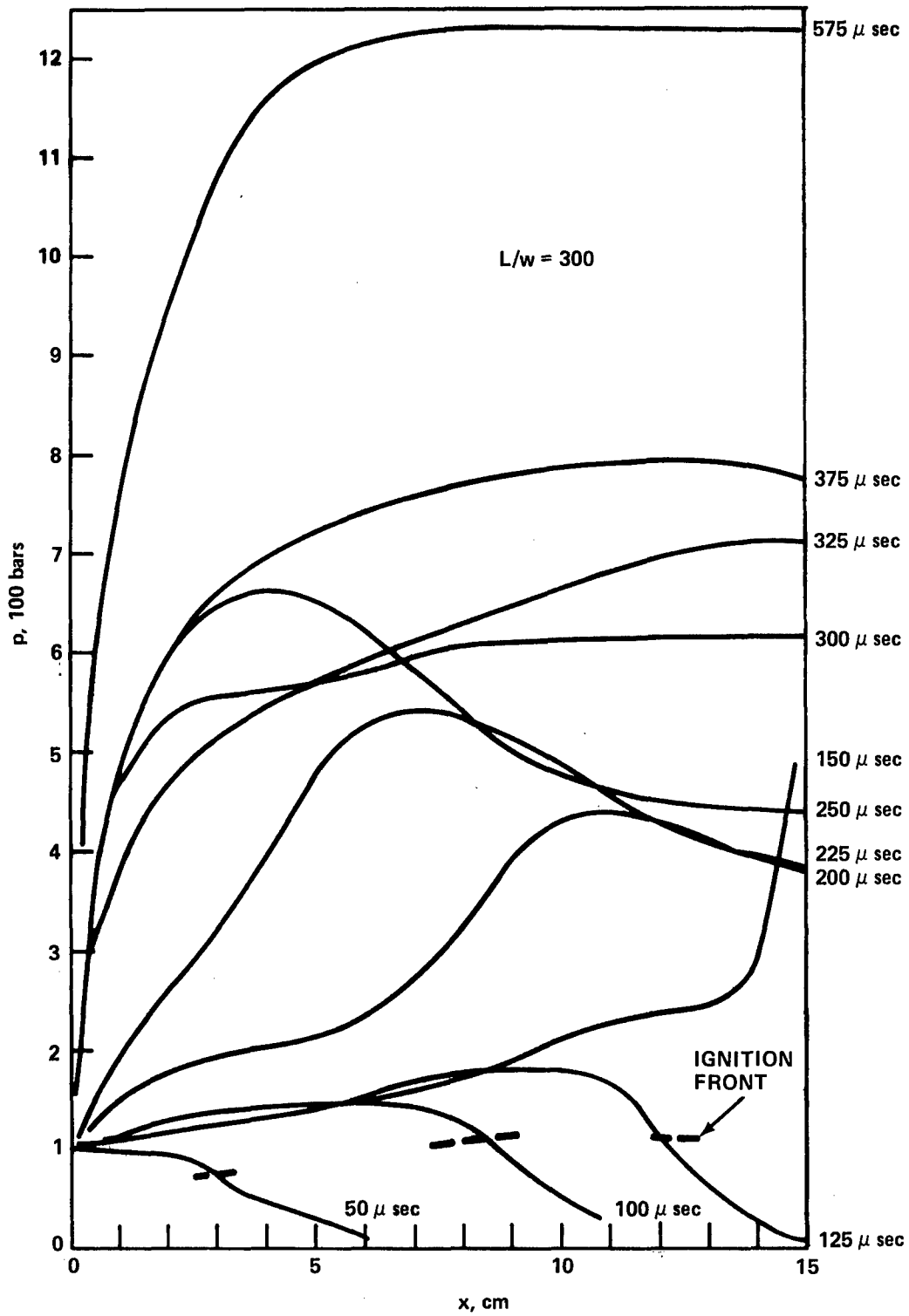


FIGURE 7 PRESSURE PROFILES --- LOWER IGNITION TEMPERATURE THAN THE BASELINE CASE I

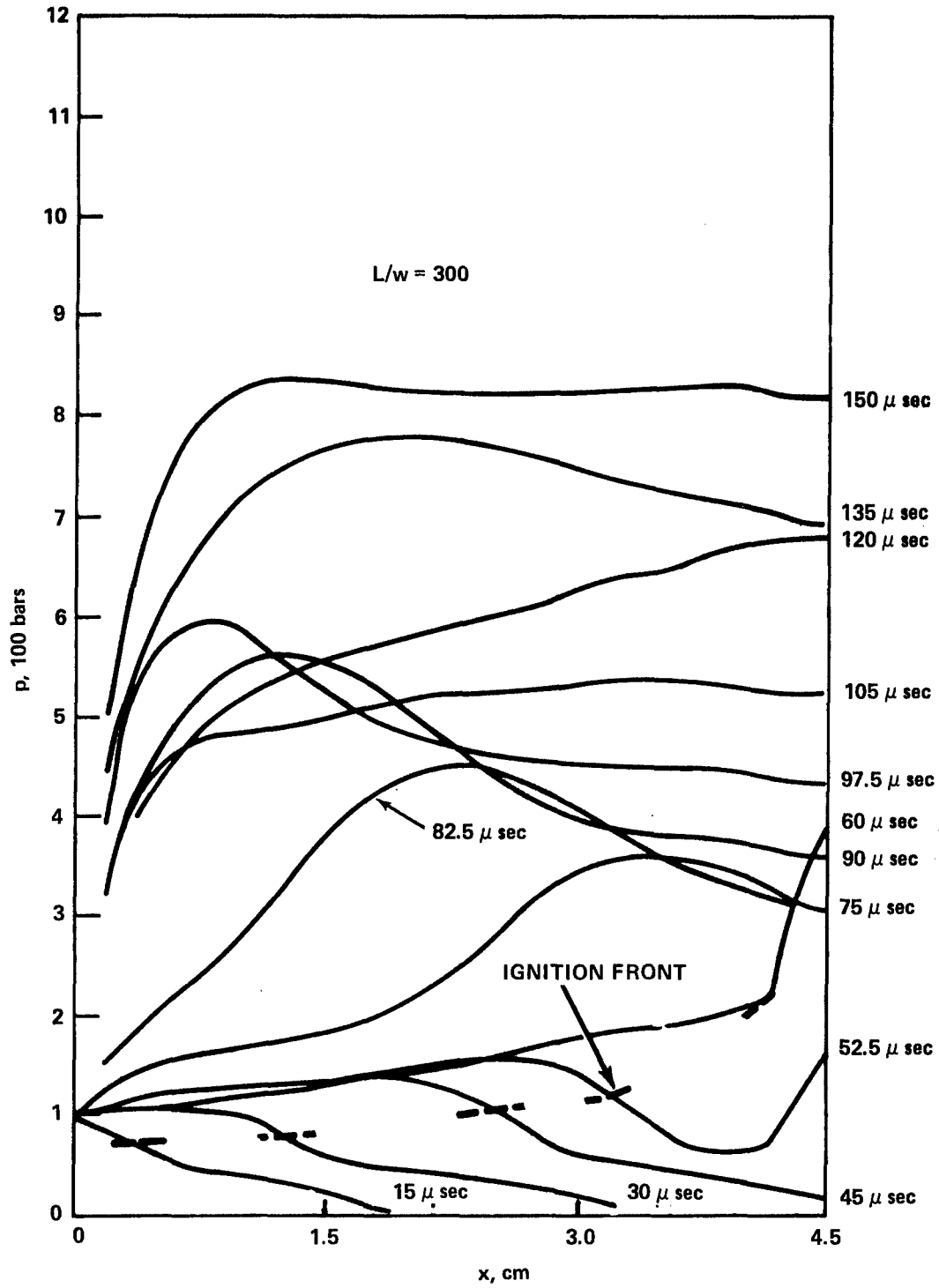


FIGURE 8 PRESSURE PROFILES --- SIMILAR-SHAPED CRACK AS THE BASELINE CASE I BUT 3/10 TIMES SMALLER

A crack of length, L , and width, W , is sandwiched between two propellant slabs of thickness of $z/2$ each which are backed by rigid walls. If z is small enough, for example, of the order of 1 cm, so that the wave in the propellant propagates laterally in a much shorter time than the characteristic time of the crack combustion, a quasi-equilibrium approximation can be introduced in calculating propellant deformation. With a propellant bulk modulus, K , neglecting any viscoelastic effect, one can estimate the change in the propellant thickness,

$$\Delta z = - z \frac{p}{K}$$

where p is the pressure in the crack. The Kuo code was modified to include this effect.

Normally, in large rocket motors it is difficult to achieve a condition such as shown in Fig. 9, with a single crack and z will be normally larger than 1 cm. As z increases, Δz becomes larger thus making the width of the crack larger. This reduces the magnitude of the peak pressure achievable in the crack combustion. However, the above condition can be qualitatively achieved in parallel cracks of equal lengths and equal widths.

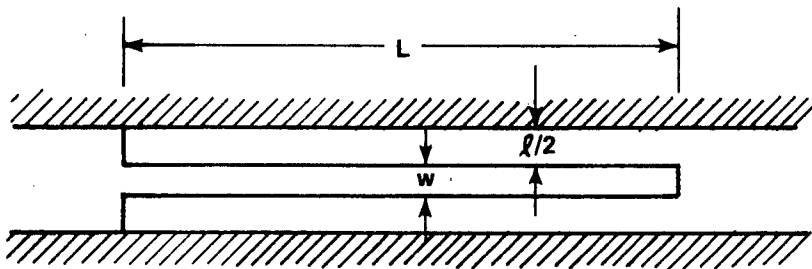


FIGURE 9 IDEALIZED SINGLE CRACK GEOMETRY IN MULTIPLE CRACK SITUATION

Since a large z decreases the maximum pressure in the crack, for the purpose of studying the possibility of obtaining high pressure for shock initiation of detonation in the propellants, the smallest value of z was examined. With the crack length, $L = 15.05$ cm and the width, $W = 150$ μ m, a value of 0.5 cm for z was investigated. With a solid particle size of the order of 200 μ m, it is difficult to conceive that any propellant thickness, z , less than 0.5 cm between many parallel cracks can be structurally strong. Weak propellants will granulate. Once the propellant is granulated, crack combustion model is no longer applicable, and convective combustion in granular, porous bed should be studied instead. Convective combustion in a granular bed is beyond the scope of this report.

The result for the case, after modification of Kuo's model, $z = 0.5$ cm, $K = 600$ Kpsi is shown in Fig. 10. It can be compared with Fig. 6 (no deformation). Propagation of the initial compression wave into the crack is almost identical in both cases at early times due to the relatively low pressure (small propellant deformation). The ignition of the propellant is achieved at the leading edge of the compression wave as before.

At later times (>175 μ sec), the cases differ. In the non-deforming case (Fig. 6), the pressurization is extremely rapid and a slow-down of the pressurization is not observed. In the deforming case (Fig. 10), a maximum pressure is observed near 400 μ sec, after which the pressure decreases. The peak pressure (at 400 μ sec) is about 5 kbars. If this pressure is maintained long enough, some propellants may react chemically at hot spots.

ROUGH SURFACE, HIGH BURNING RATES

Thus far, the study has concentrated on cracks of relatively smooth surface. However, in view of the small crack width (of the order of magnitude of some of the larger particles in the propellant), it is expected that any given crack would have rough surfaces. The effect of the rough surface is twofold: it retards the flow through large drag forces and it forms a larger burning surface area once the propellant is ignited. Many small cracks branching sideways from the main crack may also exist. These would certainly increase the available burning surface area and thereby increase pressurization in the main crack.

Exact analysis of the above situation would be difficult and time consuming. Instead, a simplistic approach was taken to account for the effects of surface roughness and many small branching cracks. To simulate the situation, the burning rate was increased by an arbitrary factor, α , while the regression rate was kept as before. This would have the same effect as having α times larger burning surface area with the same crack width. Therefore, the result of this computation would be expected to produce more severe pressurization than that of just higher burning rate with correspondingly higher regression rate (wider crack would result from faster burning). Since here the major concern is on the worst possible condition achievable in propellant crack burning, the latter can be ignored in this study.

The results of computations for values of $\alpha = 2$ and $\alpha = 3$ are shown in Fig. 11 and Fig. 12. Compared with Fig. 10 ($\alpha = 1$), it may be noted that the maximum pressure has a roughly linear functional relationship to values of α , for the range considered. A simple mass balance equation (gas generation due to burning vs gas escape through the crack opening) also confirms this rough linear relationship (not shown here).

The pressure peak observed in Fig. 12 is high enough and has a long enough duration to cause some propellants to transit to detonation. A higher α value would worsen the situation. However, this higher value of α means very extensive cross-cracking in a multiple crack area. The analysis performed here would become less effective for this case and probably a convective burning analysis in granular beds would be better employed for this purpose.

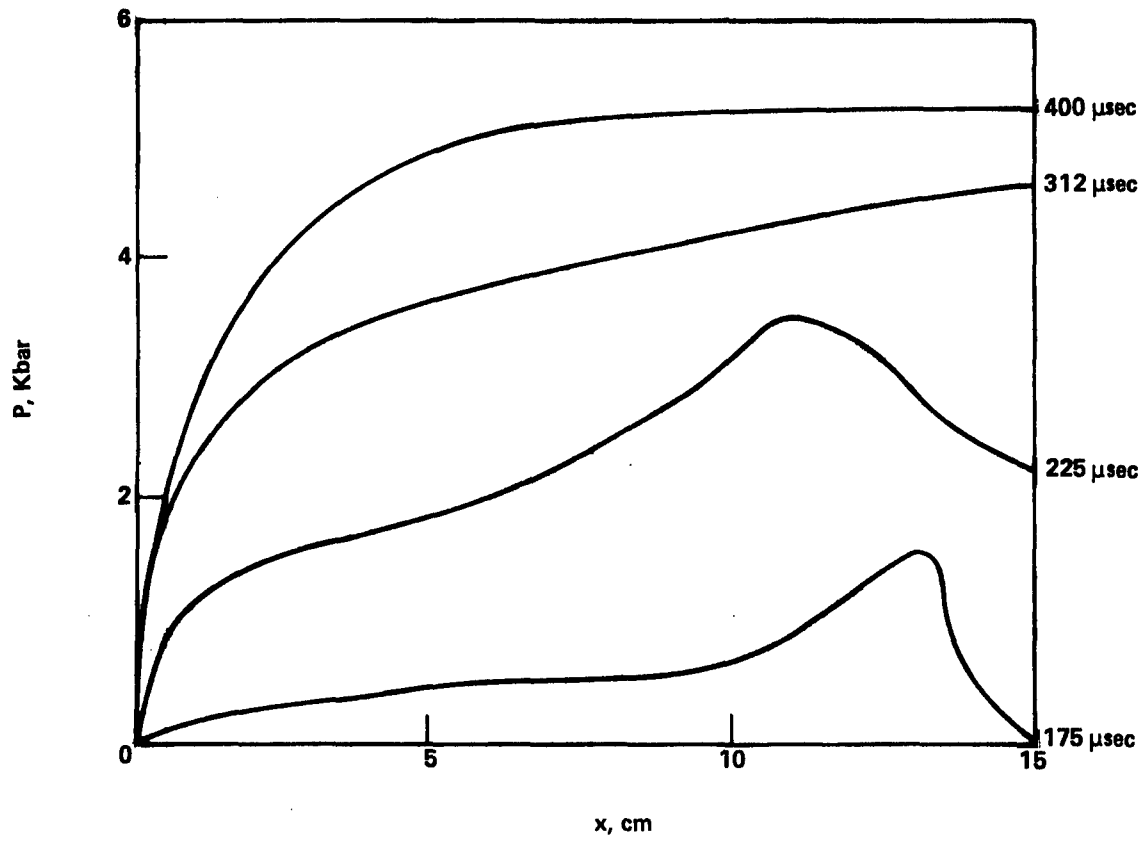


FIGURE 10 PRESSURE-DISTANCE PROFILE AT VARIOUS TIMES WITH PROPELLANT DEFORMATION

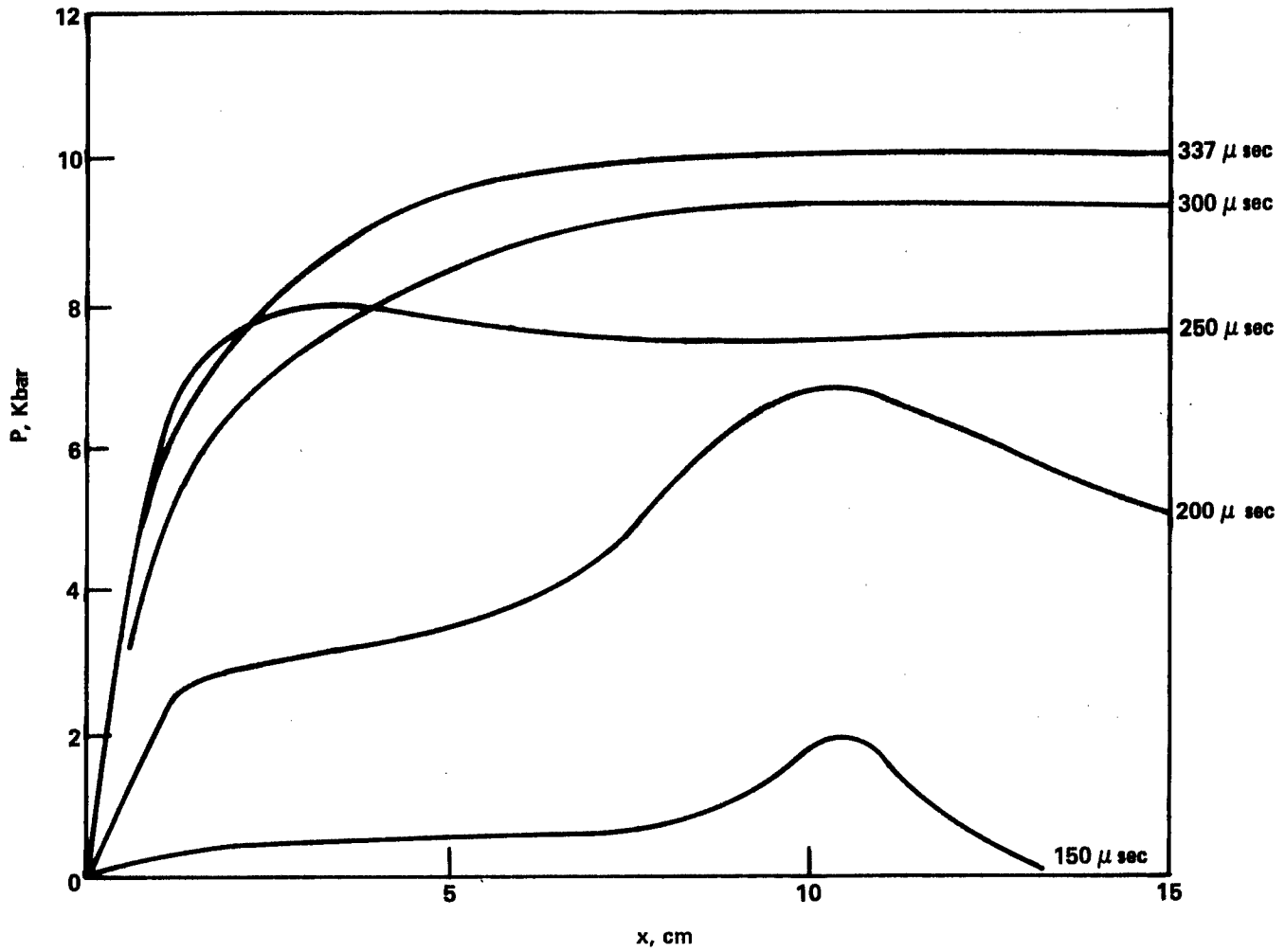
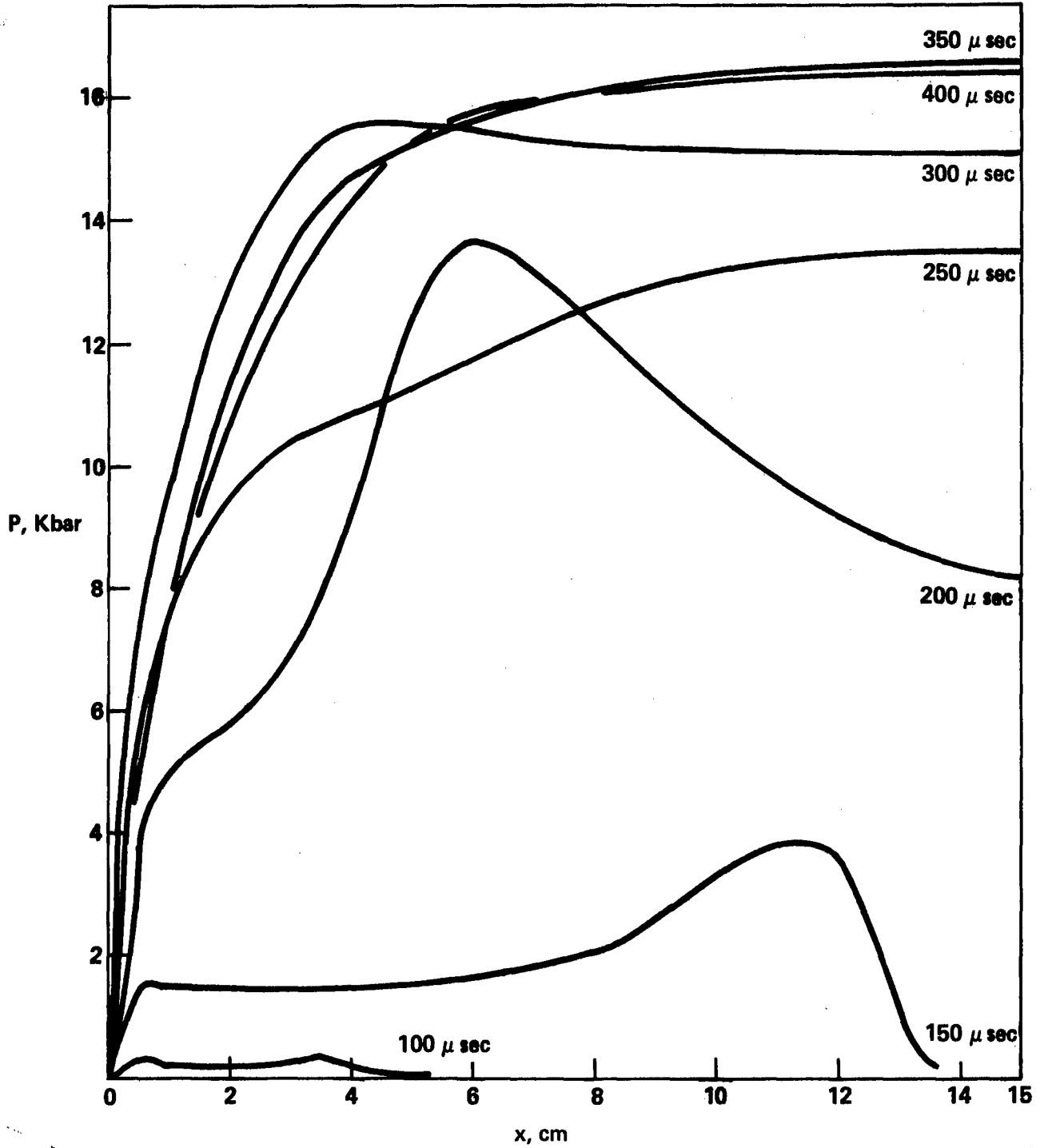


FIGURE 11 PRESSURE PROFILE WITH PROPELLANT DEFORMATION, $\alpha = 2$

FIGURE 12 PRESSURE PROFILE WITH PROPELLANT DEFORMATION, $\alpha = 3$

CONCLUSIONS

Fundamental mechanisms in crack combustion processes were examined to determine the possibility of obtaining high enough pressure to cause a transition to detonation. Several parameters were tested for their effects on the pressurization in cracks. They are summarized as follows.

1. The crack has to be an embedded one or a suddenly created one to generate high pressure in the crack.
2. The ratio of the crack length to width is an important parameter. At higher values of this ratio the length and the width must be considered separately.
3. The propellant thickness, z , between multiple parallel cracks is important.
4. The factor α , which reflects the amount of surface area available for combustion in cracks shows an almost linear relationship with the peak pressure attainable in the crack in a multiple parallel network.
5. Among propellants with the same exponent for burning rate expression, propellants with larger branching cracks with lower absolute burning rate would generate higher pressure in the cracks than propellants of smooth surface with higher burning rate.
6. Ignition criterion is the least important of the parameters studied.
7. Among the parameters discussed above, some are limited in their values to be considered realistic in the current study. The propellant thickness, z , cannot become too small, nor can the degree of the crack be too extensive; otherwise the situation no longer represents a single crack combustion process. Rather, it must be studied as a granular bed combustion process.
8. Peak pressure high enough to cause propellants to transit to detonation has not been observed in isolated smooth, short cracks, but only in long, rough cracks in a multiple crack situation with very thin propellant layers in between cracks.
9. Finally, experimental verification of the predictions is desired in order to test the assumptions used in this model and to provide more definitive directions for future studies. Also, information on the nature of real motor cracks should be provided to guide further investigation.

REFERENCES

1. Kincaid, J. F. and Jacobs, S. J., "The Fundamentals of High Energy Propellant Safety," Report No. 10342.1 SP-20 CON., Dept. of Navy, Strategic Systems Project Office, 1975.
2. Anderson, J. M., Thacher, H. H. and Wetherell, R. B., "Trident Motor Detonation Studies: An Overview," Presented at the 15th JANNAF Combustion Meeting, Rhode Island, 1978.
3. Hopkins, B. D., Peterson, N. L., Beckstead, M. W., Pilcher, D. T. and Butcher, A. G., "Mathematical Modeling of the DDT Process," Presented at the 15th JANNAF Combustion Meeting, Rhode Island, 1978.
4. Forest, C. A., "Numerical Modeling of the Deflagration-to-Detonation Transition," Presented at the 15th JANNAF Combustion Meeting, Rhode Island, 1978.
5. Prentice, J. L., "Onset of Convective Combustion: Flashdown in Solid Propellants," Presented at the 15th JANNAF Combustion Meeting, Rhode Island, 1978.
6. Jensen, R. C., "Investigation of High Velocity Impact Initiated Detonations," Presented at the 15th JANNAF Combustion Meeting, Rhode Island, 1978.
7. Belyaev, A. F., Bobolev, F. K., Korotkov, A. I., Sulimov, A. A., and Chuiko, G. V., Transition From Deflagration to Detonation In Condensed Explosives, Israel Program for Scientific Translations, Jerusalem, 1975.
8. Kuo, K. K., Chen, A. T., Davis, T. R., "Convective Burning in Solid Propellant Cracks," AIAA J., Vol. 16, No. 6, 1978.
9. Belyaev, A. T., Korotkov, A. I., Kulimov, A. A., Sukoyan, M. K. and Obmenin, A. V., "Development of Combustion in an Isolated Pore," Combustion, Explosion and Shock Waves, Vol. 5.

APPENDIX A
CRACK COMBUSTION CODE (KUO)

Kuo's crack combustion code is described in a simplified form in the following.

Basic Assumptions

The following basic assumptions are used in the theoretical model:

1. All chemical reactions occur near the propellant crack surface, in a combustion zone that is so thin that it can be considered as a plane. That is, the thickness of the combustion zone above the propellant surface is much smaller than the gap width in the propellant crack.
2. Rate processes at the propellant surface are quasisteady in the sense that the characteristic times associated with the gaseous flame and preheated propellant are short compared to that of the pressure transient variation.
3. The gases flowing in the propellant crack obey the Calusius or Noble-Abel equation of state. This dense gas relation can adequately describe the departure from the ideal gas law at high pressures.
4. The bulk flow in the pore is one-dimensional. Recent experiments conducted by Kuo et al.^{A-1} have revealed that the one-dimensional assumption is appropriate for flow in cracks when the pressure gradient along the crack is greater than a critical value, which normally is extremely small.
5. The compressibility of the solid propellant is neglected. The change of port area in propellant cracks is solely due to the propellant surface regression.

Theoretical Modeling

To describe the gas-phase behavior inside a solid-propellant crack, the mass, momentum, and energy equation in unsteady, quasi-one-dimensional forms have been developed based upon the balance of fluxes in a control volume within the propellant crack.

The mass conservation equation is

$$\frac{\partial (\rho A_p)}{\partial t} + \frac{\partial (\rho u A_p)}{\partial x} = r_b \rho_p r_b^2 \quad (1)$$

The momentum conservation equation is

$$\frac{\partial}{\partial t} (\rho A_p u) + \frac{\partial}{\partial x} (\rho A_p u^2) = - A_p \frac{\partial P}{\partial x} - p_w \tau_w \cos \theta_w - (\rho_{pr} r_b p_b) V_{gf} \sin \theta_w \quad (2)$$

The energy conservation equation written in terms of the total stored energy (internal and kinetic) per unit mass, E , is

$$\begin{aligned} \frac{\partial}{\partial t} (\rho A_p E) + \frac{\partial}{\partial x} (\rho A_p u E) = \\ - \frac{\partial}{\partial x} (A_p p u) + \rho_{pr} r_b p_b h_f \\ - \bar{h}_{cp} p_b (T - T_{ps}) \end{aligned} \quad (3)$$

After rearranging the conservation equations, a set of three governing equations is obtained, i.e., velocity-variation, temperature-variation, and pressure-variation equations. These three governing equations are first-order, coupled, inhomogeneous, and nonlinear partial differential equations. The unknowns that vary strongly with respect to the spatial variables are gas temperature, pressure, velocity, and the temperatures at the propellant surface and inert wall. There are other unknown parameters that vary weakly with respect to spatial variables. These parameters include the port area of the crack, the burning rate of the propellant, the convective heat transfer and friction coefficients, the gas flow angle, the local blowing velocity normal to the propellant surface, and the burning perimeter at various locations along the crack.

To solve all the unknowns mentioned above, additional equations and boundary conditions together with some physical input functions must be specified. The propellant surface temperature at a fixed location along the crack before the attainment of ignition is calculated from the solid-phase heat conduction equation which is written in the unsteady one-dimensional form

$$\frac{\partial T_{pr}(t,y)}{\partial t} = \alpha_{pr} \frac{\partial^2 T_{pr}(t,y)}{\partial y^2} \quad (4)$$

where the length variable y is measured perpendicular to the local propellant crack surface. The initial and boundary conditions are

$$T_{pr}(0,y) = T_{pi} \quad (5)$$

$$T_{pr}(t, \infty) = T_{pi} \quad (6)$$

$$\frac{\partial T_{pr}}{\partial y}(t, 0) = - \frac{\bar{h}_c(t)}{\lambda_{pr}} \{T(t) - T_{ps}(t)\} \quad (7)$$

The heat conduction equation is solved either by using an integral method employing a third-order polynomial or by direct numerical solution of Eqs. (4-7) with variable mesh size in the subsurface.

For the gas phase, the Nobel-Abel equation is used for the equation of state:

$$P(1/\rho - b) = RT \quad (8)$$

For the solid phase, the statement of a constant density for the solid propellant serves as the equation of state.

The expression for the local convective heat-transfer coefficient, \bar{h}_c , is deduced from the conventional Dittus-Boelter correlation for turbulent flow in pipes.^{A-2} Variation of the physical properties of the gas across the boundary layer is considered by evaluating the properties at an average film temperature, T_{af} . Before local ignition $\bar{h}_{cp} = \bar{h}_{cw} = \bar{h}_c$, whereas after local ignition $\bar{h}_{cp} = 0$ and $\bar{h}_{cw} = \bar{h}_c$. The Prandtl number used in the Dittus-Boelter correlation is calculated from Svehla's equation.^{A-3} The correlation for the friction coefficient used in this study is the modified form of the well-known Coelbrook formula,^{A-4} which is discussed in Reference A-2. Zero wall friction is assumed at the burning surface inside the crack due to large friction attenuation caused by the surface blowing.

In the absence of a more adequate erosive burning-rate expression, the Lenoir-Robillard^{A-5} burning-rate formula is used to account for erosive burning effect. After T_{ps} is solved, a simplified ignition temperature criterion is used to determine the burning condition of the solid propellant along the crack. To avoid the step function change in burning rate, a two-temperature criterion is used to achieve full ignition with a finite time interval; when T_{ps} is equal to T_{cpi} , the propellant starts to gasify. As soon as T_{ps} reaches T_{ign} , the full ignition condition is reached.

The initial conditions required for the solution of the system of governing equations are

$$u(0, x) = u_j \quad T(0, x) = T_j \quad P(0, x) = P_j \quad (9)$$

where u_j , T_j , and P_j are the initial velocity, temperature, and pressure in the propellant crack.

The number of boundary conditions required depends upon the flow direction and Mach number at the opening of the crack. When the gas in the rocket chamber flows subsonically into the propellant crack, two boundary conditions at the opening of the propellant crack are specified to represent the interface conditions at the crack entrance; and one boundary condition at the closed end of the propellant crack is specified to indicate that the gas velocity is zero. In the mathematical form, they are represented as follows:

$$P(t,0) = P_c(t) \quad T(t,0) = T_c(t) \quad u(t,x_L) = 0 \quad (10)$$

When the flow of the gas out of the crack is subsonic, two boundary conditions are specified. They are written as

$$P(t,0) = P_c(t) \quad u(t,x_L) = 0 \quad (11)$$

When the outflowing gas is supersonic, only one boundary condition can be specified, that is

$$u(t,x_L) = 0 \quad (12)$$

To solve the system of governing equations with a second-order numerical scheme, extraneous boundary conditions are required in addition to the physical ones. The procedure to attain these conditions is discussed in the following section.

Numerical Solution Technique

The governing equations, describing the flame-spreading and combustion processes in a propellant crack, were found to be totally hyperbolic.^{A-6} The numerical techniques developed were chosen on the basis of stability, maximum accuracy, and computational efficiency. Recently obtained experience in solving hyperbolic partial differential equations^{A-2} was utilized, and a generalized implicit scheme^{A-7} based on central differences in spacewise derivatives was chosen to solve the governing equations. A quasilinearization method, used to linearize the inhomogeneous terms in the governing equation, was combined with a stable predictor-corrector procedure.^{A-2} Finally, the governing equations, in their finite-difference form, are arranged in a block-tridiagonal matrix form,^{A-2} which allows an efficient computation.

The use of central difference formulation for all spacewise derivatives in the governing equations require six boundary conditions for the solution. This implies that, when the gas flows into the crack, three extraneous boundary conditions are required in addition to the three physical ones described by Eq. (10). The three extraneous boundary conditions are used to determine the flow velocity at the opening of the crack, and the pressure and temperature at the closed end of the crack.

When the gas flows out of the crack subsonically, in addition to the two physical boundary conditions described in Eq. (11), two extraneous boundary conditions are required at the opening of the crack for the determination of the pressure and temperature. Also, two extraneous boundary conditions are required at the closed end of the crack.

When the outflowing gas is supersonic, in addition to the physical boundary condition given by Eq. (12), three extraneous boundary conditions are needed at the opening of the crack and two other extraneous boundary conditions are needed at the tip of the crack.

These extraneous boundary conditions for the hyperbolic system of governing equations are derived from the compatibility relations at the boundaries. The relations are obtained by transforming the governing equations using the method of characteristics.^{A-8} The compatibility relations together with the physical boundary condition form a closed system to determine the velocity, temperature, and pressure at both ends of the crack.

NOMENCLATURE

A_p	= cross-sectional area of the crack, cm^2
b	= co-volume, cm^3/g
E	= total stored energy, cal/g
\bar{h}_c	= local convective heat-transfer coefficient, $\text{cal}/\text{cm}^2\text{-s-K}$
\bar{h}_{cp}	= local convective heat-transfer coefficient over the propellant surface, $\text{cal}/\text{cm}^2\text{-s-K}$
h_j	= enthalpy of combustion gas at adiabatic flame temperature, cal/g
b	= burning perimeter, cm
p	= static pressure, g_f/cm^2
R	= specific gas constant for the combustion gases, $\text{g}_f\text{-cm/g-K}$
r_b	= burning rate of the solid propellant, including the erosive burning contribution, cm/s
T	= temperature (without subscript, static gas temperature), K
T_f	= adiabatic flame temperature of the solid propellant, K
T_{pt}	= initial propellant temperature, K
T_{ps}	= propellant surface temperature, K
t	= time, s
u	= gas velocity, cm/s
V_{gf}	= velocity of propellant gas at the burning surface, cm/s
x	= axial distance from propellant crack opening, cm
x_t	= position at the end of crack, cm

NOMENCLATURE (Cont.)

- y = perpendicular distance from the propellant surface into the solid, cm
- α = thermal diffusivity, cm^2/s
- λ = thermal conductivity, $\text{cal}/\text{cm-s-K}$
- ρ = density (without subscript, gas density), g/cm^3
- θ_n = angle measured, in a counterclockwise direction, at the lower side of the propellant, degree
- p_b = burning perimeter, cm
- p_w = wetted perimeter of the port, cm

Subscripts

- i = initial value
- pr = solid propellant (condensed phase)
- c = rocket chamber

REFERENCES

- A-1 Kuo, K. K., Chen, A. T., and Davis, T. T., "Transient Flame Spreading and Combustion Processes inside a Solid Propellant Crack," AIAA Paper 77-14, AIAA 15th Aerospace Sciences Meeting, Jan. 1977.
- A-2 Peretz, A., Kuo, K. K., Caveny, L. H., and Summerfield, M., "Starting Transient of Solid-Propellant Rocket Motors with High Internal Gas Velocities," AIAA Journal, Vol. 11, Dec. 1973, pp. 1719-1727.
- A-3 Svehla, R. A., "Estimated Viscosities and Thermal Conductivities of Gases at High Temperatures," NASA TR R-132, 1962.
- A-4 Colebrook, C. F., "Turbulent Flow in Pipes with Particular Reference to the Transition Region Between the Smooth and Rough Pipe Laws," Journal of the Institute of Civil Engineers, Vol. 11, 1938-39, pp. 133-156.
- A-5 Lenoir, J. M. and Robillard, G., "A Mathematical Method to Predict the Effects of Erosive Burning in Solid Propellant Rockets," 6th Symposium (Int.) on Combustion, 1956, pp. 663-667.
- A-6 Courant, R., and Hilbert, D., Methods of Mathematical Physics, Vol. 2, Interscience Publishers, New York, July 1966, pp. 407-550.
- A-7 Kuo, K. K., "Theory of Flame Front Propagation in Porous Propellant Charges under Confinement," Ph.D. Thesis, AMS Report T-1000, Princeton University, Princeton, N. H., Aug. 1971.
- A-8 Richtmyer, R. D., and Morton, D. W., Difference Methods for Initial-Value Problems, Interscience Publishers, New York, 1967.

DISTRIBUTION

	<u>Copies</u>		<u>Copies</u>
Chief of Naval Material Washington, DC 20360	1	Office of Naval Technology Attn: MAT-07P (J. Enig) Department of the Navy 800 North Quincy Street Arlington, VA 22217	1
Commander Naval Air Systems Command Attn: AIR-350	1		
AIR-330	1	Commander Naval Weapons Center Attn: Code 556	1
Department of the Navy Washington, DC 20361		Technical Library	1
Commander Naval Sea Systems Command Attn: SEA-09G32	2	Code 32052 (L. Smith)	1
SEA-03B	1	Code 388 (R. L. Derr)	1
SEA-62R	1	Code 388 (T. Boggs)	1
SEA-62R2	1	Code 383 (H. D. Mallory)	1
SEA-62R3	1	China Lake, CA 93555	
SEA-62R32	1	Director Naval Research Laboratory Attn: Technical Information	2
SEA-64E	1	Section	
Department of the Navy Washington, DC 20362		Washington, DC 20375	
Director Strategic Systems Project Office (PM-1) Attn: SP-273 (R. M. Kinert)	1	Naval Plant Representative Office Strategic Systems Project Office Lockheed Missiles and Space Company Attn: SPL-332 (R. H. Guay)	1
SP-27311 (E. L. Throckmorton, Jr.)	1	P. O. Box 504 Sunnyvale, CA 94088	
John F. Kincaid	1	Redstone Scientific Information Center U. S. Army Missile Command Attn: Chief, Documents	2
Department of the Navy Washington, DC 20376		Redstone Arsenal, AL 35809	
Chief of Naval Research Attn: Rear Admiral A. J. Baciocco	1	Commanding Officer Army Armament Research and Development Command Energetic Materials Division Attn: Louis Avrami, DRDAR-LCE	1
ONR-473 (R. Miller)	1	Dover, NJ 07801	
ONR-741 (Technical Library)	1		
Department of the Navy 800 North Quincy Street Arlington, VA 22217			

DISTRIBUTION (Cont.)

	<u>Copies</u>		<u>Copies</u>
Director Applied Physics Laboratory Attn: Library Johns Hopkins Road Laurel, MD 20810	1	Pennsylvania State University Department of Mechanical Engineering Attn: K. Kuo University Park, PA 16802	1
Defense Technical Information Center Cameron Station Alexandria, VA 22314	12	Ballistic Research Laboratory Attn: N. Gerri P. Howe R. Frey D. Kooker C. Nelson Aberdeen Proving Ground, MD 21005	1 1 1 1 1
Lawrence Livermore National Laboratory University of California Attn: E. James E. Lee P. O. Box 808 Livermore, California 94550	1 1	Hercules Incorporated, Bacchus Works Attn: B. Hopkins Library 100-H D. Caldwell J. Thacher P. O. Box 98 Magna, UT 84044	1 1 2 1
Sandia Laboratories Attn: J. Nunziato R. Setchell P. O. Box 5800 Albuquerque, NM 87115	1 1	Professor H. Krier A&A Engineering Department 101 Transportation Building University of Illinois Urbana, IL 61801	1
Director Los Alamos National Laboratory Attn: Library B. G. Craig C. Forest P.O. Box 1663 Los Alamos, NM 87544	1 1 1	Chemical Propulsion Information Agency The Johns Hopkins University Applied Physics Laboratory Johns Hopkins Road Laurel, MD 20810	1
Rohm and Haas Company Huntsville Defense Contract Office Attn: H. M. Shuey Arthur Murray Building 723-A Arcadia Circle Huntsville, AL 35801	1	ITT Research Institute Attn: H. S. Napadensky 10 West 35th Street Chicago, IL 60616	1
Princeton Combustion Research Laboratories, Inc. Attn: M. Summerfield 1041 U.S. Highway One North Princeton, NJ 08540	1	Brigham Young University Department of Chemical Engineering Attn: Dr. M. W. Beckstead Provo, UT 84601	1
		Library of Congress Attn: Gift and Exchange Division Washington, DC 20540	4